Quaternion Feedback for Spacecraft Large Angle Maneuvers

Bong Wie* and Peter M. Barba†
Ford Aerospace & Communications Corporation, Palo Alto, California

This paper presents the stability and control analysis for large angle feedback reorientation maneuvers using reaction jets. The strapdown inertial reference system provides spacecraft attitude changes in terms of quaternions. Reaction jets with pulse-width pulse-frequency modulation provide nearly proportional control torques. The use of quaternions as attitude errors for large angle feedback control is investigated. Closed-loop stability analysis for the three-axis maneuvers is performed using the Liapunov stability theorem. Unique characteristics of the quaternion feedback are discussed for single-axis motion using a phase-plane plot. The practical feasibility of a three-axis large angle feedback maneuver is demonstrated by digital simulations.

Introduction

IN many future spacecraft missions, large angle reorientation/slew maneuvers will be required. Conventional single-axis small angle feedback controls may not be adequate for the three-axis large angle maneuvers. Many open-loop schemes (see, for example, Refs. 1 and 2) have been proposed for large angle maneuvers. The purely open-loop maneuvers do not require any measurement for feedback, thus, there is no possibility of closed-loop instability. However, in practice, the open-loop schemes are sensitive to the spacecraft parameter uncertainties and the unexpected disturbances. In general, combination of feedforward (open-loop) and feedback (closed-loop) controls is desirable.

In earlier works, Mortensen[3,4] suggested the use of Cayley-Rodrigues parameters and quaternions as attitude errors for large angle feedback control. Mortensen extended the conventional linear regulator concept to the case of three-axis large angle motion. Hrastar[5] applied Mortensen's control logic to the large angle slew maneuver of an Orbiting Astronomical Observatory (OAO) spacecraft. Recently, similar feedback control logic was compared with the model-reference adaptive slew maneuver about the Euler axis.[6]

In most of the slew maneuver studies, reaction wheels have been used extensively for torquing devices. The use of on-off reaction jets for slew maneuvers is also often required. The so-called "bang-off-bang" may be the most common maneuver profile using on-off reaction jets. Rapid slew maneuver about the Euler axis using reaction jets has been investigated by D'Amario and Stubbs.[7]

In general, it is necessary to know the spacecraft attitude at all times for feedback controls. The large angle orientation can be represented by a direction cosine matrix, Euler angles, or quaternions. Quaternions,[8-10] also called Euler parameters, allow the description of the spacecraft orientation in all possible attitudes. Quaternions have no inherent goemetrical singularity as do Euler angles; there are no singularities in the kinematical differential equations as do Cayley-Rodrigues parameters; and successive rotations follow the quaternion multiplication rules. Moreover, quaternions are well suited for onboard real-time computation since only products and no trigonometric relations exist in the quaternion equations. Thus, spacecraft orientation is now commonly described in terms of quaternions (e.g., HEAO, Space Shuttle, and Galileo[11]). Development of efficient strapdown attitude algorithms is also the subject of active research.[12-14]

This paper presents the stability and control analysis of three-axis large angle feedback maneuvers for a spacecraft which has an onboard microprocessor and a strapdown inertial reference system. The rate integrating gyros operate in a pulse rebalance loop to provide incremental angle changes to the quaternion integration algorithm. The spacecraft also has Earth and sun sensors, but no star sensor. However, the Earth and sun sensors cannot be used during the large angle reorientation maneuver in this paper. Control torques are provided by pulse-width pulse-frequency modulated reaction jets. The use of quaternions as attitude errors for large angle feedback control will be investigated. Characteristics of quaternion feedback will be discussed using a phase-plane plot for single-axis motion. Closed-loop stability analysis of quaternion feedback will be performed using Liapunov's stability theorem. The practical feasibility of the large angle feedback maneuver will be demonstrated by digital simulations.

Re-orientation Maneuver Requirements

Future spacecraft systems may use an integrated high-efficiency bipropellant propulsion system for both apogee and perigee maneuvers thereby reducing Space Shuttle launch costs. The orbital maneuvers will then be performed in the three-axis stabilized mode in order to control a spacecraft with high liquid mass fraction.

One of the unique characteristics of this system is the nonspinning deployment from the Space Shuttle. Many current satellites, which are three-axis stabilized in orbit, are spin-stabilized during orbit injection. Thus, they are deployed from the Space Shuttle as spin-stabilized. However, if the spacecraft is three-axis stabilized using the gimballed main engine during perigee maneuver, then it may be beneficial to have nonspinning deployment from the Shuttle. Reaction jets with a 5-lb thrust level are being considered for three-axis attitude control of the spacecraft, see Fig. 1.

Imperfect deployment could induce an initial tipoff rotational rate which may induce large angle tumbling motion if it is not actively controlled. However, the reaction jets should be disabled until the spacecraft is separated from the Space Shuttle by 200 ft, due to the Shuttle safety requirement. The coast period without an active attitude control is about 200 s since the expected deployment rate is 1 ft/s for the spacecraft considered in this paper. During this period, the

Submitted Feb. 23, 1984; presented as Paper 84-1032 at the AIAA Dynamics Specialists Conference, Palm Springs, Calif., May 17-18, 1984; revision submitted July 13, 1984.

*Engineering Specialist, Systems Analysis Department. Member AIAA.

†Principal Engineer, Systems Analysis Department. Member AIAA.

spacecraft will coast with large attitude drift due to an initial deployment tipoff rate of 0.5 deg/s in its transverse axes (negligible in longitudinal axis). The strapdown inertial reference system must track the spacecraft's attitude drift during this coast period. After being separated from the Space Shuttle by 200 ft, the reaction jets are enabled to reorient the spacecraft to its desired attitude. Thus, the spacecraft may require a large angle reorientation maneuver up to 180 deg.

The perigee orbit injection maneuver requires a total velocity pointing error of ± 3 deg (3σ). Part of the pointing error is due to the attitude determination error which includes the bias and scale factor errors of the gyros and also the computational error of the strapdown attitude algorithm. The reorientation pointing requirement is allocated as ± 0.5 deg (3σ) which is mainly due to attitude determination errors. A functional block diagram for the attitude determination and control system is shown in Fig. 2.

Attitude Determination and Control

Consider the general case of a rigid spacecraft rotating under the influence of body-fixed torquing devices. The Euler equations of motion about the principal axes of inertia are:

$$I_1\dot{\omega}_1 + (I_3 - I_2)\omega_2\omega_3 = T_1 \tag{1a}$$

$$I_2\dot{\omega}_2 + (I_1 - I_3)\omega_1\omega_3 = T_2 \tag{1b}$$

$$I_3\dot{\omega}_3 + (I_2 - I_1)\omega_1\omega_2 = T_3 \tag{1c}$$

where $(\omega_1,\omega_2,\omega_3)$, (I_1,I_2,I_3), and (T_1,T_2,T_3) are the spacecraft angular rates, moments of inertia, and control torques about the principal axes, respectively.

Euler's rotational theorem states that the rigid-body attitude can be changed from any given orientation to any other orientation by rotating the body about an axis, called the Euler axis, that is fixed to the rigid body and stationary in inertial space. The quaternion then defines the spacecraft attitude as an Euler-axis rotation from an inertial reference frame. The four elements of quaternions are defined as

$$Q_1 = C_1\sin(\phi/2) \tag{2a}$$

$$Q_2 = C_2\sin(\phi/2) \tag{2b}$$

$$Q_3 = C_3\sin(\phi/2) \tag{2c}$$

$$Q_4 = \cos(\phi/2) \tag{2d}$$

where ϕ is the magnitude of the Euler-axis rotation and (C_1,C_2,C_3) are the direction cosines of the Euler axis relative to the inertial reference frame.

The kinematical differential equations for the quaternion are:

$$2\dot{Q}_1 = \omega_1 Q_4 - \omega_2 Q_3 + \omega_3 Q_2 \tag{3a}$$

$$2\dot{Q}_2 = \omega_1 Q_3 + \omega_2 Q_4 - \omega_3 Q_1 \tag{3b}$$

$$2\dot{Q}_3 = -\omega_1 Q_2 + \omega_2 Q_1 + \omega_3 Q_4 \tag{3c}$$

$$2\dot{Q}_4 = -\omega_1 Q_1 - \omega_2 Q_2 - \omega_3 Q_3 \tag{3d}$$

with the constraint equation of quaternion unit norm

$$Q_1^2 + Q_2^2 + Q_3^2 + Q_4^2 = 1 \tag{3e}$$

The initial condition of Q_i in Eqs. (3) defines the initial spacecraft attitude with respect to the inertial reference frame. For example, initial quaternions of (0,0,0,1) define that the spacecraft is initially aligned with the inertial reference frame.

For small attitude changes from the inertial reference frame ($Q_1 = Q_2 = Q_3 \cong 0$, $Q_4 \cong 1$), we have $2\dot{Q}_1 = \omega_1$, $2\dot{Q}_2 = \omega_2$, and $2\dot{Q}_3 = \omega_3$ from Eqs. (3). Thus, the following approximations hold for small angles: $\theta_1 = 2Q_1$, $\theta_2 = 2Q_2$, and $\theta_3 = 2Q_3$, where $(\theta_1,\theta_2,\theta_3)$ are the conventional Euler angles. For a simple rotation about the fixed Euler axis, we also have the relations: $\omega_1 = C_1\dot{\phi}$, $\omega_2 = C_2\dot{\phi}$, and $\omega_3 = C_3\dot{\phi}$, where C_1, C_2, and C_3 are constant direction cosines of the Euler axis w.r.t. the inertial reference frame.

The quaternion kinematical differential equations are linear with time-varying coefficients for known body rates. They have repeated eigenvalues at $\pm j\frac{1}{2}\sqrt{\omega_1^2 + \omega_2^2 + \omega_3^2}$. In other words, the quaternion equations are neutrally stable for any value of angular rate input. This property may cause some difficulty in the numerical integration of the quaternion equations. All explicit numerical methods which are suitable for real-time computation have stability boundaries that do not include the imaginary axis except the origin. Therefore, any truncation or roundoff errors introduced in the computation, in general will not die out. The strapdown attitude algorithm to be implemented in the onboard microprocessor will be discussed later.

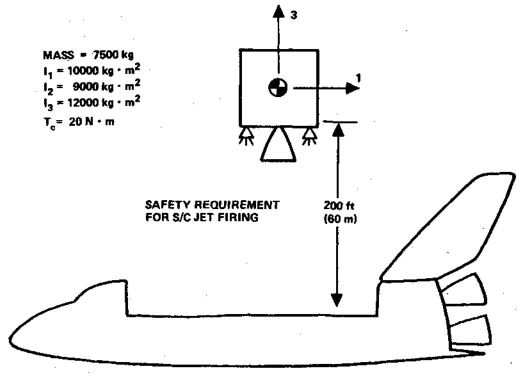

Fig. 1 Nonspinning spacecraft deployment from the Space Shuttle.

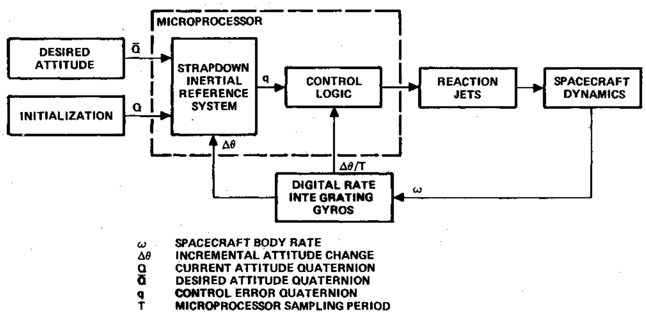

Fig. 2 Attitude determination and control.

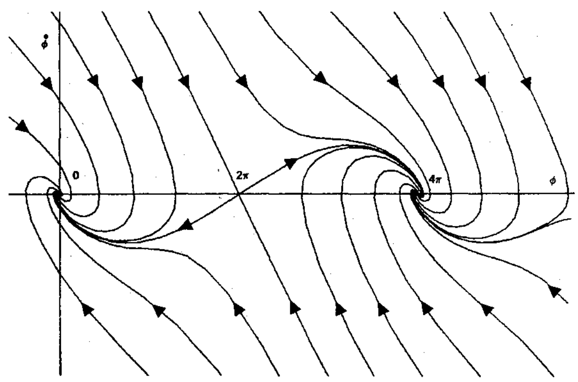

Fig. 3 Phase plane plot for single-axis rotation.

The quaternion feedback control laws to be considered in this paper are:

Control law 1:

$$T_1 = -T_c[Kq_1 + K_1\omega_1] \tag{4a}$$

$$T_2 = -T_c[Kq_2 + K_2\omega_2] \tag{4b}$$

$$T_3 = -T_c[Kq_3 + K_3\omega_3] \tag{4c}$$

Control law 2:

$$T_1 = -T_c[Kq_1/q_4^3 + K_1\omega_1] \tag{5a}$$

$$T_2 = -T_c[Kq_2/q_4^3 + K_2\omega_2] \tag{5b}$$

$$T_3 = -T_c[Kq_3/q_4^3 + K_3\omega_3] \tag{5c}$$

Control law 3:

$$T_1 = -T_c[\mathrm{sgn}(q_4)Kq_1 + K_1\omega_1] \tag{6a}$$

$$T_2 = -T_c[\mathrm{sgn}(q_4)Kq_2 + K_2\omega_2] \tag{6b}$$

$$T_3 = -T_c[\mathrm{sgn}(q_4)Kq_3 + K_3\omega_3] \tag{6c}$$

where

$$\begin{bmatrix} q_1 \\ q_2 \\ q_3 \\ q_4 \end{bmatrix} = \begin{bmatrix} \bar{Q}_4 & \bar{Q}_3 & -\bar{Q}_2 & -\bar{Q}_1 \\ -\bar{Q}_3 & \bar{Q}_4 & \bar{Q}_1 & -\bar{Q}_2 \\ \bar{Q}_2 & -\bar{Q}_1 & \bar{Q}_4 & -\bar{Q}_3 \\ \bar{Q}_1 & \bar{Q}_2 & \bar{Q}_3 & \bar{Q}_4 \end{bmatrix} \begin{bmatrix} Q_1 \\ Q_2 \\ Q_3 \\ Q_4 \end{bmatrix} \tag{7}$$

where q_i is the control error quaternion, $\bar{Q}_i$ the commanded attitude quaternion w.r.t. the commanded attitude. For a special case of attitude quaternion w.r.t. the inertial reference frame, Q_i the currently estimated spacecraft quaternion w.r.t. the inertial reference frame, and T_c the control torque level of reaction jets; K and K_i are positive control gains.

Equation (7) is the result of successive quaternion rotations using the quaternion multiplications and inversion rules. The control error quaternion q_i is simply the current spacecraft attitude quaternion w.r.t. the commanded attitide. For a special case of attitude regulation w.r.t. the inertial reference frame, the commanded quaternion is (0,0,0,1). Then the currently estimated spacecraft quaternion simply becomes the control error quaternion. Also for an inertially fixed commanded attitude quaternion, Q_i becomes the control error quaternion with reinitialization using Eq. (7).

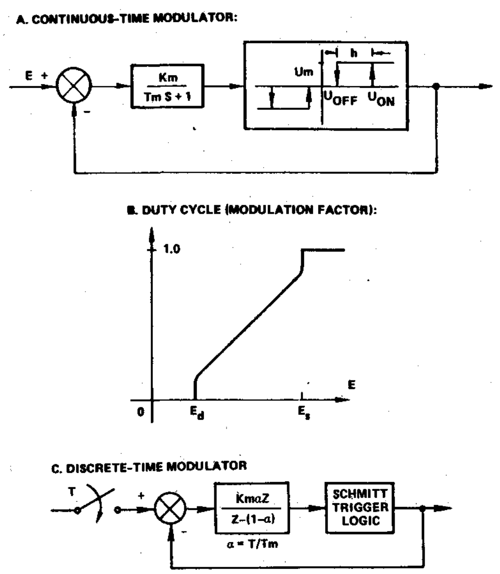

Fig. 4 PWPF modulator.

The three control laws presented above are analogous to a conventional feedback control law in that the control torque is a function of position and rate.[15] For $q_4 > 0$, control laws 1 and 3 are identical, however, they have completely different closed-loop behaviors for $q_4 < 0$, which will be discussed later by introducing Liapunov asymptotic stability. The pulse-width pulse-frequency modulator has been considered as a linear device in the above equations. The theoretical background of such assumption will also be discussed later.

A Special Case of Single-Axis Large Angle Rotation

Some physical insight of the quaternion feedback control laws can be obtained by considering a single-axis large angle rotation. The closed-loop equations with control laws 1, 2, and 3 then can be written as:

Control law 1:

$$I\ddot{\phi} + T_cK_R\dot{\phi} + T_cK\sin(\phi/2) = 0 \tag{8a}$$

Control law 2:

$$I\ddot{\phi} + T_cK_R\dot{\phi} + T_cK\sin(\phi/2)/\cos^3(\phi/2) = 0 \tag{8b}$$

Control law 3:

$$I\ddot{\phi} + T_cK_R\dot{\phi} + T_cK\mathrm{sgn}[\cos(\phi/2)]\sin(\phi/2) = 0 \tag{8c}$$

where ϕ is the single-axis attitude error, and attitude control about the origin is considered here.

We notice that the closed-loop equations have linear viscous damping and nonlinear "spring" terms. Equation (8a) is similar to the nonlinear equation of a simple pendulum with viscous damping. Thus, the closed-loop behavior of control law 1 is very much similar to the nonlinear behavior of a simple pendulum with large angle motion.[18,19]

A typical phase-plane plot for control law 1, Eq. (8a), is shown in Fig. 3. Every trajectory, other than the separatrices going into the saddle points, ultimately approaches one of the stable equilibrium points. The number of full rotations before reaching the equilibrium point depends on the initial magnitude of rate. As to be expected, the greater the initial rate beyond certain limits, the greater the number of full rotations before reaching the stable equilibrium point.

The separatrices come into the saddle points at $\phi = \pm 2\pi$, $\pm 6\pi, \ldots$, whereupon the spacecraft has the choice of rotating either in the same direction or backward. Such saddle points in Fig. 3 correspond to the upside-down position of a simple pendulum problem (but with $\phi = 180$ deg). The stable equilibrium points are $\phi = 0$, $\pm 4\pi, \ldots$, as can be seen from Fig. 3. For control law 1, the saddle points correspond to $Q_4 = -1$; the stable equilibrium points correspond to $Q_4 = 1$. It is important to note that both the saddle and stable points in Fig. 3 correspond to the physically identical orientation.

Similar phase-plane plots for Eqs. (8b) and (8c) can also be constructed, which have saddle points at $\phi = \pm\pi$, $\pm 3\pi, \ldots$, and stable equilibrium points at $\phi = 0$, $\pm 2\pi$, $\pm 4\pi, \ldots$. Simple phase-plane interpretation discussed here may be useful for gaining physical insight into three-axis large angle motion.

Liapunov Nonlinear Stability Analysis

Closed-loop stability is the major concern in any feedback control system design. If the system is linear and time-invariant, many stability criteria are available. If the system is nonlinear, such stability criteria do not apply. For small angles, the system with the control laws discussed previously becomes the classical single-axis position and rate feedback, which is well known to be closed-loop stable. For single-axis large angle motion, the stability can be easily studied using phase-plane plot, as discussed before. However, for three-axis large angle motion, it is not obvious whether such control laws can provide global closed-loop stability or not.

The Liapunov second method (also known as the Liapunov direct method) to be used in this paper may be the most general method for the determination of stability of nonlinear systems. Using the Liapunov second method, we can determine the stability of a system without solving the state equations. Only the inertially fixed commanded attitude quaternion is considered here.

First, consider control law 1. After substituting Eqs. (4) and (7) into the Euler equations, multiply each equation by ω_1, ω_2, and ω_3, respectively. After multiplying each of Eqs. (3) by $T_cK(Q_1-\bar{Q}_1)$, $T_cK(Q_2-\bar{Q}_2)$, $T_cK(Q_3-\bar{Q}_3)$, and $T_cK(Q_4-\bar{Q}_4)$, respectively, add these equations to the previously modified Euler equations. We can then define

$$\dot{V} \equiv \sum_{i=1}^{3} I_i\dot{\omega}_i\omega_i + 2T_cK\sum_{i=1}^{4}\dot{Q}_i(Q_i-\bar{Q}_i) = -T_c\sum_{i=1}^{3}K_i\omega_i^2 < 0 \tag{9}$$

A positive definite Liapunov function, V, then can be found as

$$V = \tfrac{1}{2}\sum_{i=1}^{3} I_i\omega_i^2 + T_cK\sum_{i=1}^{4}(Q_i-\bar{Q}_i)^2 > 0 \tag{10}$$

Thus, the closed-loop system with control law 1 is *asymptotically stable in the large,* since $\dot{V}<0$

$$\lim_{t\to\infty} V(x) = 0 \quad \text{and} \quad \lim_{\|x\|\to\infty} V(x) = \infty$$

where x is the state vector. The stable equilibrium point with this control law is: $\omega_1=\omega_2=\omega_3=0$ and $Q_i=\bar{Q}_i$ $(i=1,2,3,4)$. Thus, this control law reorients the spacecraft to the desired attitude from an arbitrary initial orientation. Similarly, for control law 2, substitute Eqs. (5) and (7) into the Euler equations, then multiply each equation by $2\omega_1$, $2\omega_2$, and $2\omega_3$, respectively. Multiply each of Eqs. (3) by $-T_cK(Q_i+2\bar{Q}_i/q_4^3)$, $i=1,2,3,4$. Add these equations to the previously modified Euler equations to define

$$\dot{V} \equiv 2\sum_{i=1}^{3} I_i\dot{\omega}_i\omega_i - 2T_cK\sum_{i=1}^{4}\dot{Q}_i(Q_i+\bar{Q}_i) + 2T_cK(1-2q_4^{-3})\dot{q}_4$$

$$= -2T_c\sum_{i=1}^{3}K_i\omega_i^2 < 0 \tag{11}$$

A positive definite Liapunov function, V, then can be found as

$$V = \sum_{i=1}^{3} I_i\omega_i^2 - T_cK\sum_{i=1}^{4}(Q_i+\bar{Q}_i)^2 + 2T_cK(q_4+q_4^{-2})$$

$$= \sum_{i=1}^{3} I_i\omega_i^2 + 2T_cK(-1+q_4^{-2}) > 0 \quad (\text{since } |q_4|\le 1) \tag{12}$$

Thus, the closed-loop system with control law 2 is also *asymptotically stable in the large,* since $\dot{V}<0$

$$\lim_{t\to\infty} V(x) = 0 \quad \text{and} \quad \lim_{\|x\|\to\infty} V(x) = \infty$$

Note that there exist two asymptotically stable equilibrium points with the second control law: $Q_i=\pm\bar{Q}_i$, $i=1,2,3,4$. The equilibrium point with $Q_i=-\bar{Q}_i$ is physically the same orientation with $Q_i=\bar{Q}_i$. For an initial error of $q_4<0$, the second control law becomes positive position feedback; it provides a shorter path and least action to reach the desired equilibrium point.

For small angles, the three control laws provide the same linear performance. However, for large angles, they provide significantly different performances. The q_4 becomes zero as the Euler rotation angle ϕ becomes 180 deg. Thus, the second control law can result in a nearly infinite control signal for certain initial orientations. The first control law, however, never results in such a situation since the magnitude of q_i $(i=1,2,3)$ is never greater than one. For an initial orientation with $q_4<0$, however, the second control law provides more efficient reorientation maneuvers, as discussed previously. The third control law also provides an efficient reorientation maneuver for an arbitrary initial orientation without the possibility of an infinite control signal.

In the previous stability analysis, the position gain has been restricted to be the same in each axis. Such a restriction resulted in an easy determination of the Liapunov function. It does not mean that the control laws discussed previously become unstable without such a constraint. Asymptotic stability in the large has not yet been proven when a different position gain is used in each axis. Although nothing can be concluded about global stability from the stability of linearized system, it is known that when a linearized system is asymptotically stable, the nonlinear system from which it is derived is also asymptotically stable.[18]

Consider control law 1 with different position gain in each axis. When the closed-loop system is linearized near the

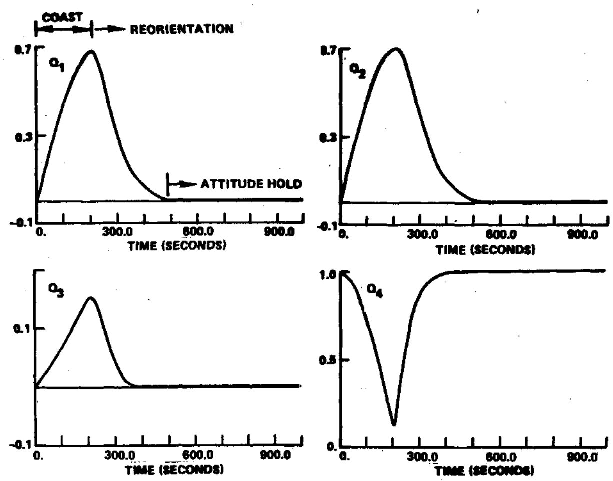

Fig. 5 Digital simulation results (quaternions).

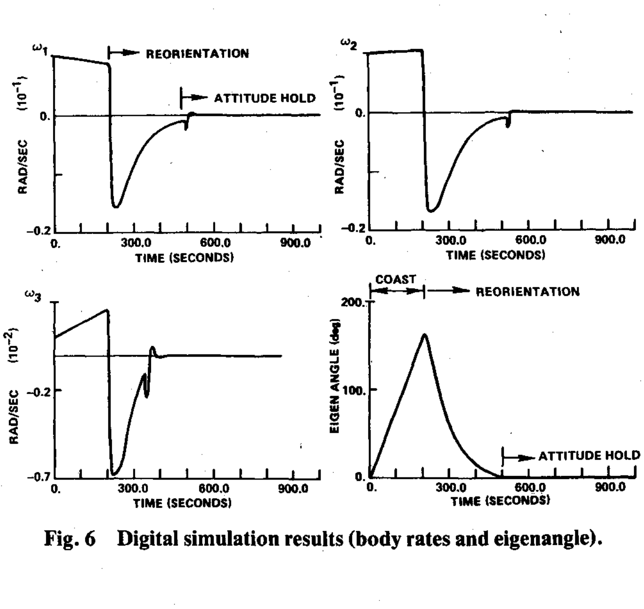

Fig. 6 Digital simulation results (body rates and eigenangle).

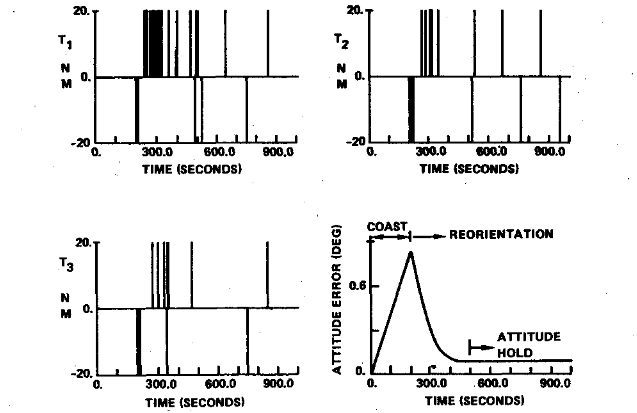

Fig. 7 Digital simulation results (thruster activity and attitude error).

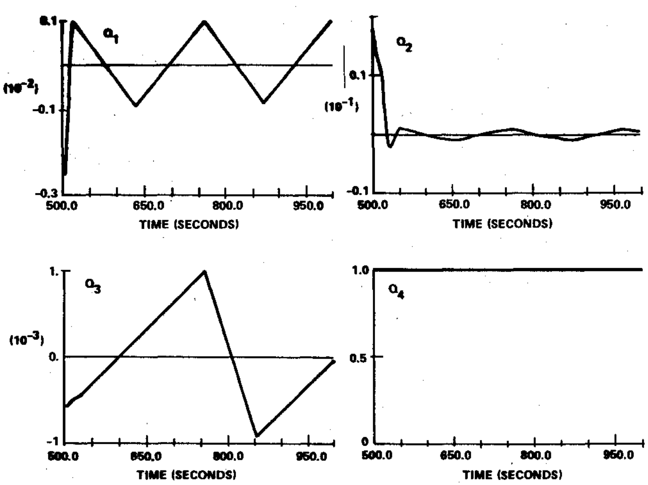

Fig. 8 Digital simulation results (steady-state limit cycle).

equilibrium point, the result is three uncoupled linear second-order systems. These are easily proven asymptotically stable by conventional methods. Thus, the original nonlinear system is also asymptotically stable with different position gain in each axis.

For a special case of three-axis large angle motion, but with *small* angular rate, the global stability of the control laws (1, 2, 3) with different position gain in each axis can also be easily proved by the Liapunov stability theorem. Feedforward time-varying slew command can also be generated to achieve smooth and time- and/or fuel-optimal maneuvers.[6,7,17,21] In this paper, we consider only feedback reorientation maneuvers with simple step command.

PWPF Modulator

The pulse-width pulse-frequency (PWPF) modulator has been assumed as a linear device in the previous analysis. In this section, the theoretical background of such assumption will be discussed briefly. The PWPF modulator shown in Fig. 4a produces a pulse command sequence to the thruster valve by adjusting the pulse width and pulse frequency. In the linear range, the average torque produced equals the demanded torque input. The pulse width is very short and the pulse frequency is usually fast compared to the spacecraft rigid-body dynamics. The static characteristics of the modulator are good enough for rigid spacecraft attitude control, while the dynamic characteristics of the modulator are needed for flexible spacecraft attitude control (e.g., Ref. 16).

With a constant input, the PWPF modulator drives the thruster valve with an on-off pulse sequence having a nearly linear duty cycle with input amplitude. The duty cycle or modulation factor is defined as the average output of the modulator. The static characteristics of the continuous-time modulator for a constant input E are as follows:

$$\text{Minimum pulse width} \qquad \equiv T_m h / K_m U_m \tag{13a}$$

$$\text{Internal deadband} \qquad E_d = U_{\text{on}} / K_m \tag{13b}$$

$$\text{Saturation level} \qquad E_s = U_m + U_{\text{off}} / K_m \tag{13c}$$

where $h = U_{\text{on}} - U_{\text{off}}$ = hysteresis width. The U_{on}, U_{off}, K_m, and T_m are the design prameters of the modulator. A typical plot of the duty cycle which is nearly linear over the range above deadband and below saturation is shown in Fig. 4b.

A discrete-time PWPF modulator for microprocessor implementation is also shown in Fig. 4c. The modulator gets an input signal every T s and causes pulse command updates every $T/4$ s. Equation (13a) derived for a continuous-time modulator becomes invalid for a discrete-time modulator. An equality relation for the discrete-time modulator with $T/4$ s minimum pulse width can be obtained as

$$h < K_m U_m T / 4 T_m < 2 U_{\text{on}} \tag{14}$$

where T is the microprocessor sampling period.

The modulator provides an effective loop gain reduction at lower frequency and additional phase lag at higher frequency. The phase lag of the modulator decreases as the time constant T_m decreases. Detailed describing function analysis of the modulator can be found in Ref. 16.

Quaternion Integration for Strapdown Inertial Reference

There are a number of numerical methods available for solving the quaternion equations. Methods which can be applied to the strapdown attitude algorithms include Taylor series expansion,[5,17] the rotation vector concept,[11-13] Runge-Kutta algorithms, and the state transition matrix.[14] Of these methods, the Taylor series expansion lends itself well to the use of an incremental angle output from the digital rate integrating gyros.

The strapdown attitude algorithm using the fourth-order Taylor series expansion, which requires only the current information from the gyros, can be written as[17]:

$$Q_i(t+T) = Q_i(t)$$

$$\underbrace{+R_i(t)}_{\text{1st}} \underbrace{-D^2 Q_i(t)}_{\text{2nd}} \underbrace{-D^2 R_i(t)/3}_{\text{3rd}} \underbrace{+D^4 Q_i(t)/6}_{\text{4th order}} \tag{15}$$

where

$$D^2 = (\Delta\theta_1)^2 + (\Delta\theta_2)^2 + (\Delta\theta_3)^2$$

$$R_1 = ½[\Delta\theta_1 Q_4 - \Delta\theta_2 Q_3 + \Delta\theta_3 Q_2]$$

$$R_2 = ½[\Delta\theta_1 Q_3 + \Delta\theta_2 Q_4 - \Delta\theta_3 Q_1]$$

$$R_3 = ½[-\Delta\theta_1 Q_2 + \Delta\theta_2 Q_1 + \Delta\theta_3 Q_4]$$

$$R_4 = ½[-\Delta\theta_1 Q_1 - \Delta\theta_2 Q_2 - \Delta\theta_3 Q_4]$$

and $\Delta\theta_1$, $\Delta\theta_2$, and $\Delta\theta_3$ are the incremental angle outputs from the gyros over the quaternion integration time step, T. The body rates to be used for feedback controls are simply $\Delta\theta_i / T$.

Different strapdown attitude algorithms can also be found in Refs. 11-13. Such algorithms require the previous samples of the gyro outputs as well as the current outputs. For any algorithm, there exist computational errors due to Taylor series truncation and microprocessor finite word length. Another type of error also exists known as degradation of quaternion unit norm length. However, this error can be eliminated by normalization of the quaternion update equation. Tradeoff between algorithm complexity vs algorithm truncation and roundoff errors is generally required.

Digital Simulation

A digital simulation was used to verify the practical feasibility of large angle feedback maneuvers. The spacecraft parameters have been given in Fig. 1. The control torque level of reaction jets is assumed as 20 N-m in each axis, with negligible cross-axis coupling. The gyro has quantization of 0.9 arc sec/pulse, a residual drift rate of 0.1 deg/h, and a scale factor error of 0.5%. It was assumed that only drift bias is estimated and calibrated in the Shuttle before deployment. Thus, the scale factor error of 0.5% is relatively large and considered as the worst case. The 32-bit onboard microprocessor has a cycle time of 64 ms and a process delay of 48 ms.

The attitude determination error is defined as the difference between the true spacecraft attitude and the attitude computed from the strapdown inertial reference system using the gyros. Thus, the attitude errors consist of errors due to residual drift rate and scale factor error, and strapdown attitude update computational error. Because of a relatively fast sampling period of 64 ms, the pointing error is dominated by the gyro sensor error not by computational error. Thus, attitude update algorithm with the first-order Taylor was good enough for preliminary analysis and simulations. The true spacecraft attitude was computed by means of a fourth-order Runge-Kutta routine with an integration time step of 16 ms in double precision.

As discussed previously, control laws 1 and 3 are identical for $q_4>0$, but their closed-loop behaviors for $q_4<0$ are completely different from each other. The 360-deg orientation is unstable for control law 1, but is stable for control law 3. As the spacecraft attitude drifts, the attitude determination error increases due to the gyro scale factor error. Control law 1 reorients the spacecraft backward to 0 deg by minimizing the effect of the gyro scale factor error even for the initial condition of $q_4<0$.

The results of a typical simulation using control law 1 are shown in Figs. 5-8. The desired attitude quaternion is assumed to be (0,0,0,1). The initial body rates are: $\omega_1=\omega_2=0.53$ deg/s and $\omega_3=0.053$ deg/s. The control loop with $K=0.5$ and $K_i=200$ is enabled at $t=200$ s. Thus, for the reorientation maneuver, the initial orientation is: $Q_1=0.685$, $Q_2=0.695$, $Q_3=0.153$, and $Q_4=0.153$ with Euler rotation angle of 162 deg. Since the initial orientation is less than 180 deg, the three control laws will reorient the spacecraft backward to 0-deg equilibrium point. In this paper, only the simulation results using control law 1 are presented.

The spacecraft quaternions shown in Fig. 5 approach the desired value in a well-behaved manner. Figure 6 shows the time histories of the body rates and the Euler rotation angles. Note that the Euler rotation angle decreases in an exponential manner. Figure 7 shows the time histories of the jet firings. The periods of acceleration and deceleration and attitude hold are evident. The jet firings are acceptable in a practical sense, although the maneuver was not "optimal" like an ideal "bang-off-bang." Total jet firing time was 50 s during the 300-s reorientation and the 500-s attitude hold mode. Figure 7 also shows some measure of spacecraft attitude determination error, which meets the pointing requirement of 0.5 deg after the reorientation maneuver. The attitude determination error increases as the spacecraft attitude drifts due to the scale factor error. Once the control loop is closed (at $t=200$ s), the pointing error decreases with an offset error. The offset error is due to the different path between the coast and the reorientation. The attitude error increases very slowly as time goes on due to the gyro drift bias.

The attitude-hold mode with $K=100$ and $K_i=200$, which is automatically initiated at the end of the maneuver, maintains the attitude of the spacecraft inside the control-loop deadband as shown in Fig. 8. The effective deadband angle was chosen to be 0.1 deg.

Conclusions

The stability and control analysis for large angle feedback reorientation maneuvers with strapdown inertial reference system have been presented. The control logic was a simple extension of the conventional feedback control to the three-axis large angle coupled motion. Some physical interpretation of quaternion feedback was given using a phase-plane plot. Liapunov's stability theorem was used to determine the global stability of the closed-loop system. The maneuver discussed in this paper was not necessarily optimal in the theoretical sense of minimum time and/or fuel. However, the closed-loop system approached the desired attitude in a well-behaved manner. Dominant pointing error source was shown to be the effect of the gyro scale factor error because of the nature of large angle maneuvers.

References

[1] Barba, P.M. and Aubrun, J.N., "Satellite Attitude Acquisition by Momentum Transfer," *AIAA Journal*, Vol. 14, Oct. 1976, pp. 1382-1386.

[2] Vadali, S.R. and Junkins, J.L., "Spacecraft Large Angle Rotational Maneuvers with Optimal Momentum Transfer," *Journal of Astronautical Sciences*, Vol. XXXI, No, 2, April-June 1983, pp. 217-235.

[3] Mortensen, R.E., "On Systems for Automatic Control of the Rotation of a Rigid Body," Electronics Research Lab., University of California, Berkeley, Calif., Rept. 63-23, Nov. 27, 1963; also, *Journal of Applied Mechanics*, March 1965, pp. 228-230.

[4] Mortensen, R.E., "A Globally Stable Linear Attitude Regulator," *International Journal of Control*, Vol. 8, No. 3, 1968, pp. 297-302.

[5] Hrastar, J., "Attitude Control of a Spacecraft with a Strapdown Inertial Reference System and Onboard Computer," NASA TN D-5959, Sept. 1970.

[6] Ven den Bosch, P.P.J. et al., "An Adaptive Attitude Control System for Large Angle Slew Maneuvers," IFAC Automatic Control in Space, the Netherlands, 1982.

[7] D'Amario, L.A. and Stubbs, G.S., "A New Single-Axis Autopilot for Rapid Spacecraft Attitude Maneuvers," *Journal of Guidance and Control*, Vol. 2, July-Aug. 1979, pp. 339-346.

[8] Margulies, G., "On Real Four-Parameter Representations of Satellite Attitude Motions," Mathematical Analysis Dept., Philco Western Lab., Palo Alto, Calif., Rept. 52, Sept. 1963.

[9] Kane, T.R., Likins, P.W., and Levinson, D.A., *Spacecraft Dynamics*, McGraw-Hill Book Co., New York, 1983.

[10] Ickes, B.P., "A New Method for Performing Control System Attitude Computation Using Quaternions," *AIAA Journal*, Vol. 8, Jan. 1970, pp. 13-17.

[11] Wong, E.C. and Breckenridge, W.G., "Inertial Attitude Determination for a Dual-Spin Planetary Spacecraft," *Journal of Guidance, Control and Dynamics*, Vol. 6, Nov.-Dec. 1983.

[12] Miller, R.B., "A New Strapdown Attitude Algorithm," *Journal of Guidance, Control and Dynamics*, Vol. 6, July-Aug. 1983, pp. 287-291.

[13] McKern, R. and Musoff, H., "Strapdown Attitude Algorithms from a Geometric Viewpoint," *Journal of Guidance and Control*, Vol. 4, Nov.-Dec. 1981, pp. 657-661.

[14] Mayo, R.A., "Relative Quaternion State Transition Relation," *Journal of Guidance and Control*, Vol. 2, Jan.-Feb. 1979, pp. 44-48.

[15] Bryson, A.E. Jr., *Stabilization and Control of Flight Vehicles*, Class Notes, Aero/Astro Dept., Stanford University, Stanford, Calif., 1983.

[16] Wie, B. and Plescia, C.T., "Attitude Stabilization of Flexible Spacecraft During Stationkeeping Maneuvers, *Journal of Guidance, Control and Dynamics*, Vol. 7, July-Aug. 1984, pp. 430-436.

[17] Cunningham, D.C. et al., "System Design of the Annular Suspension and Pointing System (ASPS)," *Proceedings of the AIAA Guidance and Control Conference*, Palo Alto, Calif., 1978.

[18] Struble, R.A., *Nonlinear Differential Equations*, McGraw-Hill Book Co., New York, 1962, pp. 131-136.

[19] Cannon, R.H., *Dynamics of Physical Systems*, McGraw-Hill Book Co., New York, 1967, pp. 355-370.

[20] Breckenridge, W.G. and Man, G.K., "Quaternions for Galileo Scan Platform Control," AAS/AIAA Astrodynamics Specialists Conference, Lake Placid, N.Y., Paper 83-321, Aug. 1983.